Asian Journal of Chemistry; Vol. 35, No. 1 (2023), 159-164

ASIAN JOURNAL OF CHEMISTRY

https://doi.org/10.14233/ajchem.2023.24022

Synthesis of Solid Polymer Blend Electrolytes Based on PVP/PAN/Ammonium Thiocyanate: Structural, Electrical, Dielectric and Electrochemical Analysis

R. Daniel[1,2], S. Janet Priscilla[1,2], S. Karthikeyan[2], S. Selvasekarapandian[3], K. Sivaji[1,*] and S. Madeswaran[4]

[1]Department of Nuclear Physics, University of Madras, Chennai-600025, India
[2]Department of Physics, Madras Christian College, Chennai-600059, India
[3]Materials Science Research Center, Coimbatore-641045, India
[4]Centre for Functional Materials, Vellore Institute of Technology, Vellore-632014, India

*Corresponding author: E-mail: sivaji@unom.ac.in

Received: 18 August 2022; *Accepted*: 10 December 2022; *Published online*: 27 December 2022; AJC-21093

In this work, a solution casting technique was used to prepare stable and free-standing films of blend polymer electrolytes composed of polyvinyl pyrrolidone (PVP) and polyacrylonitrile (PAN) complexed with ammonium thiocyanate (NH_4SCN) salt in various compositions. The physical characterization by X-ray diffraction (XRD) was performed to study the structural properties of the samples. Characteristics of these electrolytes were also examined using impedance technique, dielectric studies, transport number measurement (TNM) and linear sweep voltammetry (LSV). The results showed that cationic transport predominated in highly amorphous films. Impedance spectroscopy was utilized to determine the dependence of electrical properties on both composition and temperature. The temperature dependence of the electrical conductivity showed behaviour similar to that of Arrhenius type. It was found that the highest ion conducting polymer blend electrolyte led to lower activation energy.

Keywords: Polymer blend, Polymer electrolyte, Impedance spectroscopy, Dielectric constant, Linear sweep voltammetry.

INTRODUCTION

Due to their excellent ionic conductivity, extended lifetime, high mechanical strength and short time period for film formation, solid polymer electrolytes (SPEs) have played a crucial role in the development of contemporary electrochemical energy storage and conversion systems in recent decades [1]. A widespread interest can be attributed to the fact that these materials open the door to exciting new applications such fuel cells, electrochemical cells, rechargeable batteries, sensors and photoelectrochemical solar cells [2,3]. There are a number of methods that can be used to improve the mechanical, electrical and electrochemical properties of polymer electrolytes, which can be done by combining two polymers, adding salts and fillers [4]. The host polymer most frequently used by the researchers are polyethylene oxide (PEO) [5-7], poly(vinyl alcohol) (PVA) [8-11], chitosan (CS) [12-14] and Nafion membranes [15]. Ionic conductivity intensifiers are generated in the polymer blends through the incorporation of inorganic salts. In proton conducting polymer electrolytes, hydrogen ions serve as the charge carriers, which may be generated through the dissociation of a variety of ammonium salts [16].

Some ammonium compounds have been employed as dopants since they are good proton (H^+) donors [17,18], which include ammonium thiocyanate (NH_4SCN), ammonium nitrate (NH_4NO_3), ammonium chloride (NH_4Cl), ammonium iodide (NH_3I) and ammonium bromide (NH_3Br). This study generated a proton-conducting polyethylene by employing an NH_4SCN salt with low-lattice energy as proton source. In this research, ammonium thiocyanate (NH_4SCN) salt was doped into a polyvinyl pyrrolidone (PVP) and polyacrylonitrile (PVP-PAN) blended system at varying concentrations. For a full understanding of the structure-property interactions, the structural and electrochemical properties of PVA-PAN-based blended polyethylenes (PEs) have also been studied.

EXPERIMENTAL

Preparation of solid polymer blend electrolyte films: In this work, the polymer blend was prepared from the polyvinylpyrrolidone (PVP), polyacrylonitrile (PAN) containing ammonium thiocyanate salt (≥ 99%) as dopant and dimethylformamide as solvent. All chemicals were procured from Sigma-Aldrich and used without further purification. The PVP/PAN/NH_4SCN solid polymer blend electrolyte (SPE) films were prepared through the solution casting technique. Initially, PVP was added to the solvent (DMF) at room temperature and stirred continuously until the complete dissolution of the polymer. Then, PAN was added separately into solvent and heated at 60 ºC in order to dissolve PAN and stirred for 48 h. It was allowed to stir continuously to obtain homoge-nous mixture. Separately in various beakers, PVP-PAN mixture solutions were stirred continuously for 6 h while varying amount of NH_4SCN dopant salt, with weight percentages of salts ranging from 10 to 50 wt.% were added (Table-1). The resulting solution were transferred into uncovered Petri dishes and kept in a vacuum oven at 60 ºC for 48 h to remove the presence of solvent in the sample and to obtain completely dry SPE films. Mechanically stable and free standing membrane was obtained from this procedure. The films were allowed to dry at ambient temperature in order to obtain films free of solvents and then placed in a desiccator containing silica gel for 24 h.

TABLE-1
DESIGNATION AND COMPOSITION OF PVP-PAN WITH NH_4SCN SOLID POLYMER BLEND ELECTROLYTE (SPE) SYSTEMS

Sample code	Composition	NH_4SCN (wt.%)
PPA@10	80PVP:20PAN	10
PPA@20	80PVP:20PAN	20
PPA@30	80PVP:20PAN	30
PPA@40	80PVP:20PAN	40
PPA@50	80PVP:20PAN	50

RESULTS AND DISCUSSION

Structural (XRD) analysis: The XRD analysis was carried out on PVP:PAN system at various salt concentration (10-50 wt.%) of NH_4SCN. Fig. 1 illustrates the X-ray diffraction pattern of 80PVP:20PAN and 80PVP:20PAN:NH_4SCN blend systems at room temperature. There was an increase in the amorphous area in the blended system, as evidenced by a broadening of the peaks and a decrease in their intensities in the XRD pattern as the salt content was increased [19]. The peaks of the SPE film decrease some of their strength when the concentration of NH_4SCN increases up to 30 wt.%. This implies that the strong crystalline peaks of NH_4SCN were eliminated as a result of an unambiguous interaction between the dopant salt and the polymer blend. The emergence of certain noticeable peaks at a salt concentration of 50 wt.% may be attributed due to the recrystallization of salt. The increases in the intramolecular and intermolecular hydrogen bondings are responsible for the expansion of the amorphous phase when NH_4SCN concentration increases [20]. Therefore, the interaction between the blended polymer and the dopant salt is revealed by the decrease in the peak level and the broadening in the XRD pattern of PPA@30 electrolyte. The amorphous nature offers higher ionic conductivity and increased ionic diffusivity. The maximum DC ionic conductivity was observed in the PPA@30 electrolyte.

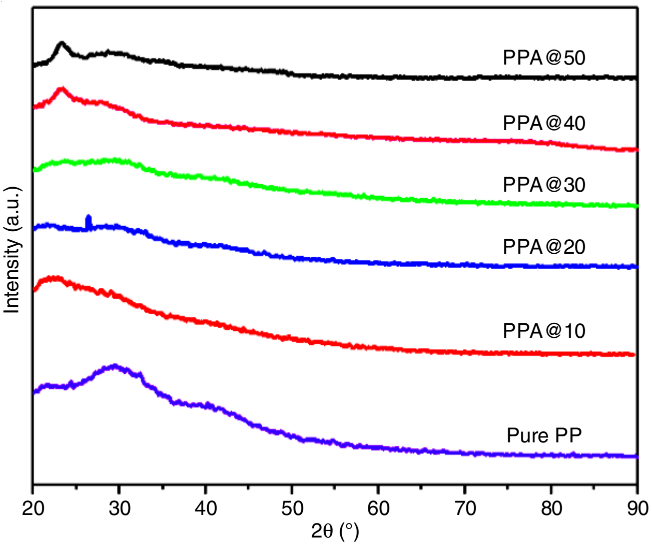

Fig. 1. XRD pattern of blend polymer electrolyte 80PVP:20PAN:NH_4SCN for various salt concentrations at room temperature

Impedance analysis: Complex impedance measurements of polymer electrolytes often show two major zones on a typical plot. A semi-circle in the high-frequency region is caused by the bulk action of electrolyte, while the spike in the low-frequency region is caused by the blocking effect of electrode [21-23], since the polymeric electrolyte membrane carries ion species. As an AC electric field is applied, ion diffusion takes place through the polymer film. Fig. 2 shows the impedance plot of blended polymer 80PVP:20PAN:NH_4SCN electrolyte films for various salt concentrations at room temperature.

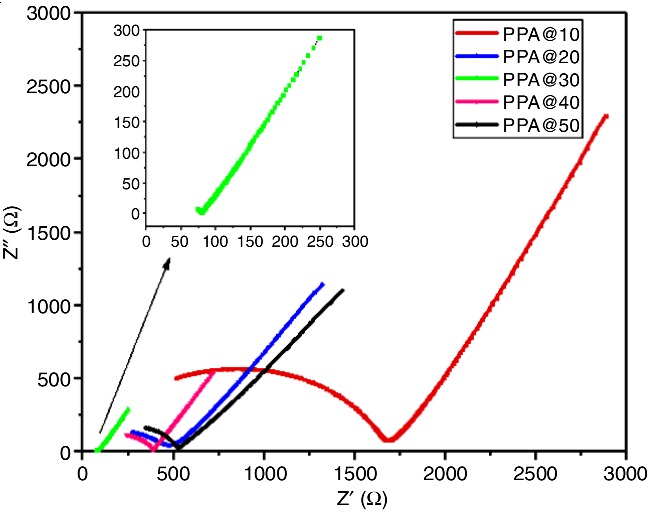

Fig. 2. Cole-Cole plot of blend polymer electrolyte 80PVP:20PAN:NH_4SCN for various salt concentrations at room temperature

It is interesting that the impedance plot at low frequency exhibit a spike inclined at an angle less than 90º indicate the existence of a rough or inhomogeneous electrode/electrolyte interface [24]. This inclination also clearly exemplifies the polarization effect within the electrolytes and the effect of the blocking electrodes [25,26]. The ionic conductivity of the blended SPE membrane can be calculated using the following equation:

TABLE-2
IONIC CONDUCTIVITY AT DIFFERENT TEMPERATURE FOR THE SPE 80PVP:20PAN:NH_4SCN (10-50 wt.%)

Sample	Ionic conductivity (10^{-3} S/cm)							
	303 K	313 K	323 K	333 K	343 K	353 K	363 K	373 K
PPA@10	0.0202	0.0291	0.0433	0.122	0.285	0.59	1.79	4.46
PPA@20	0.0935	0.2030	0.3860	0.809	1.780	3.82	9.32	17.8
PPA@30	0.6050	0.7850	1.2000	1.810	2.620	4.15	7.24	13.8
PPA@40	0.1080	0.1860	0.2590	0.406	0.798	1.72	4.50	10.60
PPA@50	0.0691	0.0936	0.1360	0.229	0.483	1.15	3.25	9.74

$$\sigma = \frac{t}{R_b A} \tag{1}$$

where t is the thickness of the electrolyte sample, A is the contact area of the electrode, R_b is the bulk resistance of the sample.

The bulk resistance (R_b) values for all the blended SPE membrane were determined from the interception of the spike line with real axis (Z′). The DC conductivities were calculated and tabulated as shown in Table-2. The highest DC conductivity value of 6.05 × 10^{-4} S cm^{-1} is obtained for the polymer blend electrolyte 80PVP:20PAN:NH_4SCN at 30 wt.% salt concentration (PPA@30) with the lowest R_b value. It is clear from the impedance plot that R_b was reduced with the increase of salt concentration NH_4SCN upto 30 wt.%. However, bulk resistance (R_b) is increased upon further addition of NH_4SCN content upto 50 wt.%. It is due to the agglomeration of ions in the blended polymer-salt mixtures, which reduces the number of mobile charge carrier resulting to a decrease in ionic conductivity of the system [27].

Temperature dependent of ionic conductivity: The linear variation of ionic conductivity of the blended polymer electrolyte for various salt concentrations with inverse of temperature over the temperature range from 303 K to 373 K is shown in Fig. 3. Least squares analysis has been used to fit the experimental data for all the polymer blend electrolytes.

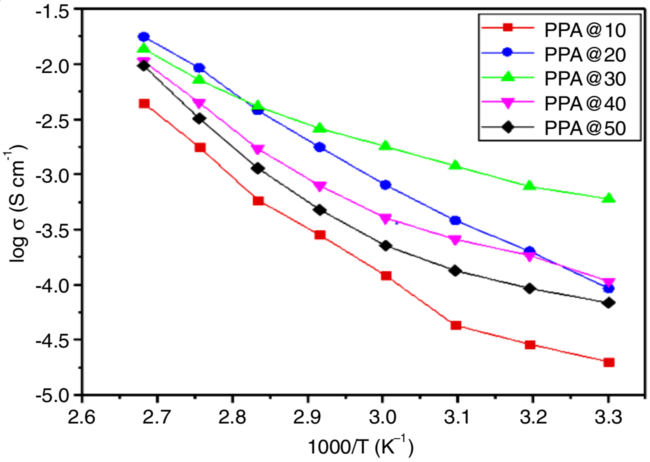

Fig. 3. Arrhenius plot of blend polymer electrolyte 80PVP:20PAN:NH_4SCN for various salt concentrations at different temperature

From Fig. 3, the ionic conductivity increases linearly with the increase in temperature. It is evident that the temperature-dependent ionic conductivity for the blended polymer electrolyte undergoes the enhancement in ionic conductivity with increase in temperature obeys Arrhenius rule [28], which is governed by the following relation:

$$\sigma = Ae^{\left(\frac{-E_a}{K_B T}\right)} \tag{2}$$

where E_a is the activation energy, A is a pre-exponential factor, K_B is the Boltzmann constant and T is the absolute temperature. The activation energies (E_a) for the blended polymer samples were calculated and tabulated in Table-3. It is apparent that as the concentration of ions in the polymer electrolyte increases which leads to a decrease in the energy barrier to ion transport as a result, the activation energy E_a decreases. Hence, it is observed that polymer electrolyte 80PVP:20PAN:30 wt.% NH_4SCN has a highest ionic conductivity of 6.05 × 10^{-4} S cm^{-1} at 303 K and lower activation energy of 0.1856 eV compared to other polymer samples.

TABLE-3
ACTIVATION ENERGY (E_a) AND RELAXATION
TIME FOR THE BLEND POLYMER ELECTROLYTES

Sample	Activation energy (eV)	Relaxation time (s)
PPA@10	0.3352	1.092 × 10^{-5}
PPA@20	0.3196	4.115 × 10^{-6}
PPA@30	0.1856	8.418 × 10^{-7}
PPA@40	0.2712	5.935 × 10^{-6}
PPA@50	0.2959	1.418 × 10^{-4}

Dielectric analysis: The mechanism of ion transport in a polymer-based electrolyte can be deduced from its dielectric characteristics. Using this method, the polarization effect and ion conduction behaviour in electrolyte films can be characterized. Dielectric characteristics were calculated from the dielectric parameter plots for SPE electrolytes with varying salt concentrations using the following formulae [29]:

$$\varepsilon' = \frac{Z_i}{\omega C_0 (Z_r^2 + Z_i^2)} \tag{3}$$

$$\varepsilon'' = \frac{Z_r}{\omega C_0 (Z_r^2 + Z_i^2)} \tag{4}$$

where, ω is the angular frequency of the applied filed; ε′ is the dielectric constant; ε″ is the dielectric loss and C_0 is the capacitance in vacuum.

Fig. 4a-b illustrates the frequency dependence of dielectric constant (ε′) and dielectric loss (ε″) for the polymer blend electrolyte sample 80PVP:20PAN:NH_4SCN with varying salt concentrations of NH_4SCN at room temperature. Clearly, the dielectric permittivity parameters (ε′, ε″) are at their maximum in low-frequency areas due to electrode polarization and a high

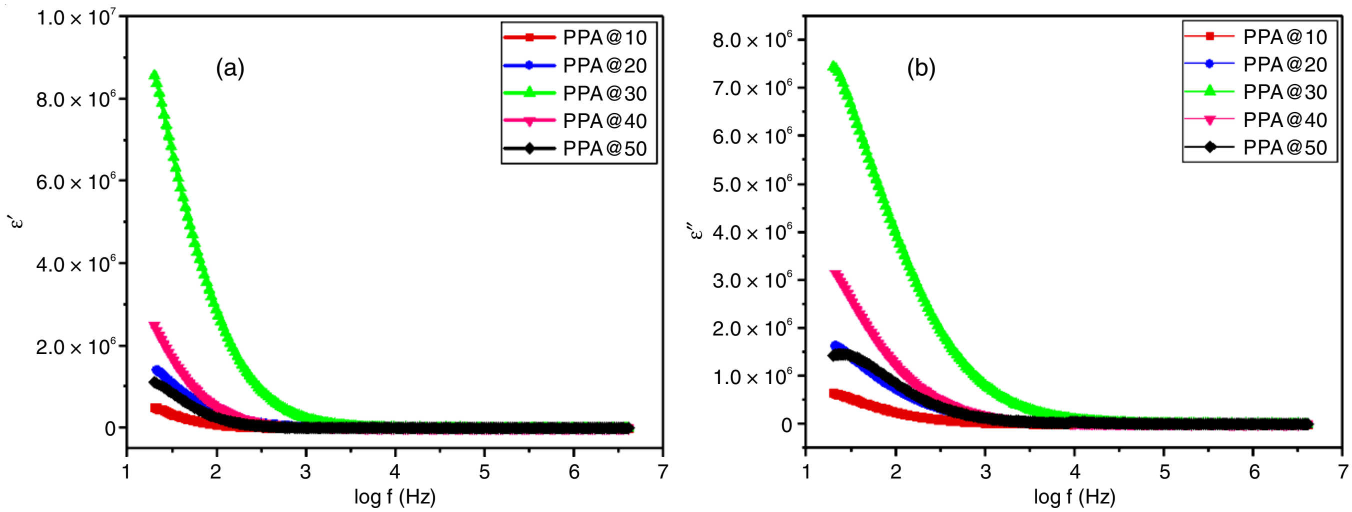

Fig. 4. Plot of (a) log f *vs.* ε' and (b) log f *vs.* ε'' of blend polymer electrolyte for various salt concentrations at room temperature

density of charge carriers [30]. In the higher frequency zone, however (> 10 kHz), the values of dielectric permittivity parameters (ε', ε'') are not considerably frequency dependant. Due to the greater number of ions and the maximum ionic conductivity, the PPA@30 polymer blend electrolyte exhibits a high value of the dielectric constant (ε') at low frequencies. Fig. 4a demonstrates that when the concentrations of doped salt grew up to 30% NH_4SCN, the value of the dielectric constant (ε') increased steadily. However, over 30 wt.%, dielectric constant (ε') decreases due to the decrease in the concentration of mobile charge carriers. In the high frequency zone, a rapid shift of the applied electric field tends to limit ion diffusion due to the relaxing of dipoles, as shown in Fig. 4b [31].

Tangent loss: The dielectric relaxation parameter of the polymer blend electrolytes can be characterized by the loss tangent spectra. The dielectric loss tangent (tan δ) is defined as:

$$\tan\delta = \frac{\varepsilon''}{\varepsilon'} \tag{5}$$

Fig. 5 shows the variation of tangent loss with angular frequency of polymer blend films for different salt concentrations of 80PVP:20PAN:NH_4SCN at room temperature. It can be observed that the peak at a characteristic frequency for polymer blend electrolyte suggests the relaxation dipole. The dielectric loss tangent peak is shifted towards the higher frequency with increasing concentration of doped salt thereby reducing the relaxation time [32].

The relaxation time were calculated from the loss tangent spectra by the relation:

$$\omega\tau = 1 \tag{6}$$

where τ is the relaxation time and ω the angular frequency of the applied external field. The relaxation time has been calculated for the polymer blend electrolytes of various NH_4SCN concentrations at room temperature and tabulated in Table-3. It is evident that the relaxation time is short for PPA@30 due to the increased mobility of ions in the polymer matrix, which is consistent with the conductivity studies indicating that the PPA@30 polymer electrolyte has a higher ionic conductivity.

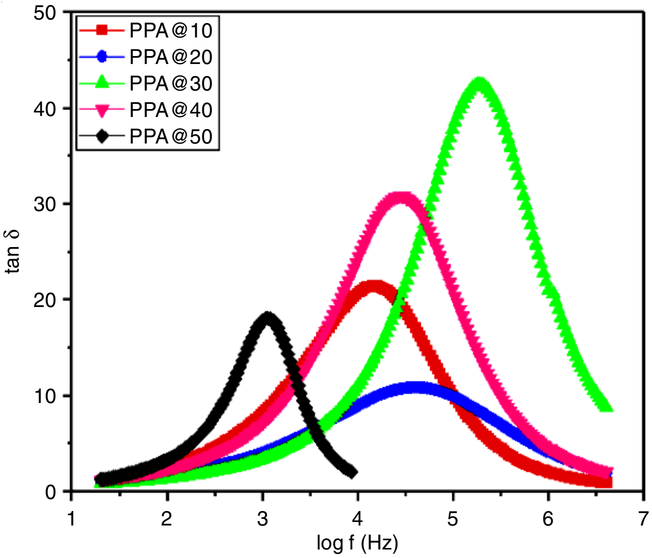

Fig. 5. Tangent loss spectra of blend polymer electrolyte 80PVP:20PAN:NH_4SCN for various salt concentration at room temperature

Transference number: Transference number measurement technique to identify the type charge species responsible for the conductivity was done by the Wagner's DC polarization technique. Fig. 6 shows the plot of polarization current *versus* time at constant voltage of 1.5 V for the highest conducting polymer electrolyte PPA@30 film.

Due to the decrease of ionic species in the electrolyte, it can be observed that the initial current declines fast with time. Once the cell reaches steady state, it is polarized and any remaining current is generated by the migration of electrons between the electrolyte-electrode surfaces [33].

The equations given below are used to determine the values of both ionic (t_{ion}) and the electronic (t_e) transference numbers.

$$t_{ion} = \frac{I_i - I_{ss}}{I_i} \tag{7}$$

$$t_e = 1 - t_i \tag{8}$$

where I_i is the initial current and I_{ss} is the steady-state current.

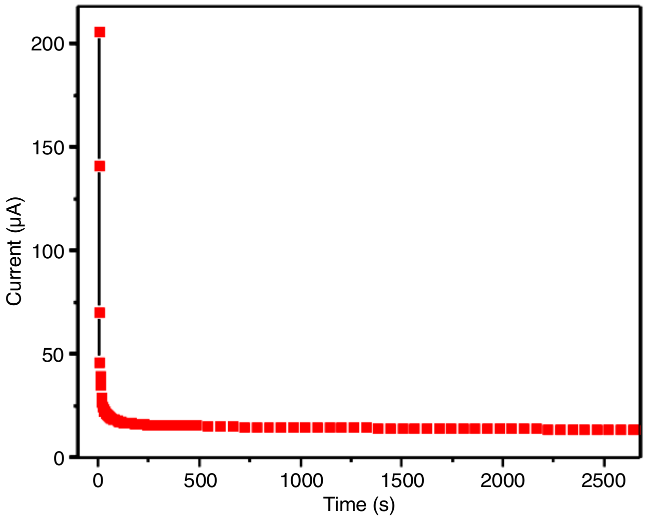

Fig. 6. Polarization curve of current *vs.* time for highest conducting blend polymer electrolyte 80PVP:20PAN:30 wt.% NH_4SCN

The ionic (t_{ion}) and electronic (t_e) transference number for the highest conductivity polymer electrolyte PPA@30 was found to be 0.976 and 0.023. It indicates that the charge transport is predominantly due to ions.

Linear sweep voltammetry (LSV): The electrochemical stability is the crucial parameter to use SPEs in energy storage device applications. By employing the linear sweep voltammetry (LSV), the electrochemical stability window of the highest conducting polymer electrolyte 80PVP:20PAN:30 wt.% NH_4SCN was investigated at the scan rate of 5 mV/s.

The LSV plot of the highest conducting polymer electrolyte film PPA@30 at room temperature is shown in Fig. 7. For the ready cell assembly with stainless steel electrodes, a decomposition voltage was measured between 0 and 5 V at a scan rate of 5 mV/s and found that the current did not increase until reached 2.55 V. At room temperature, the breakdown voltage of the polymer electrolyte was found to be 2.55 V. Above 2.55 V, current density increased dramatically because the polymer electrolyte was being broken down on the surface of electrode [34]. The decomposition voltage of 80PVP:20PAN:30 wt.% NH_4SCN blend polymer electrolyte is high enough to make it practical for usage in energy storage devices.

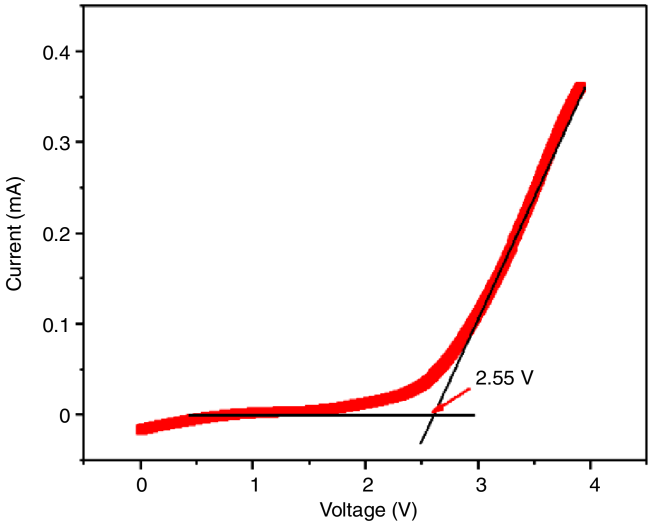

Fig. 7. Linear sweep voltammetry for highest conducting blend polymer electrolyte 80PVP:20PAN:30 wt.% NH_4SCN at room temperature

Primary proton battery: The best conducting polymer blend electrolyte, PPA@30, is employed to construct the proton battery with the cell configuration.

$$\mathrm{Zn + ZnSO_4 \cdot 7H_2O\,(anode) \| SPE \| PbO_2 + V_2O_t\,(cathode)}$$

Zinc is oxidized in proton batteries to generate Zn^{2+} ions and electrons at the anode. While the electrons move in the external circuit, Zn^{2+} ions are still present at the anode [35]. Thus, it is evident that hydrated zinc sulphate provides protons to the battery during discharge. The anodic reaction is as follows:

$$\mathrm{nZn + ZnSO_4 \cdot 7H_2O \longrightarrow}$$
$$\mathrm{Zn_{n+1}(SO_4) \cdot (7\text{–}2n)H_2O \cdot 2n(OH) + 2nH^+ + 2e^-}$$

At the cathode (positive electrode), reduction of lead oxide (PbO_2) and vanadium pentoxide (V_2O_5) occurs in the cell according to the following reactions:

$$\mathrm{PbO_2 + 4H^+ + 2e^- \longrightarrow Pb_2^+ + 2H_2O}$$

$$\mathrm{V_2O_5 + 6H^+ + 2e^- \longrightarrow 2VO_2^+ + 3H_2O}$$

The highest conducting polymer blend electrolyte was sandwiched between the anode and cathode; this fabricated cell is placed in a suitable holder as shown in Fig. 8 and the multimeter is connected across the cell to measure the open-circuit voltage (OCV). Fig. 9 shows the voltage of cell as a function of time at room temperature in open circuit condition.

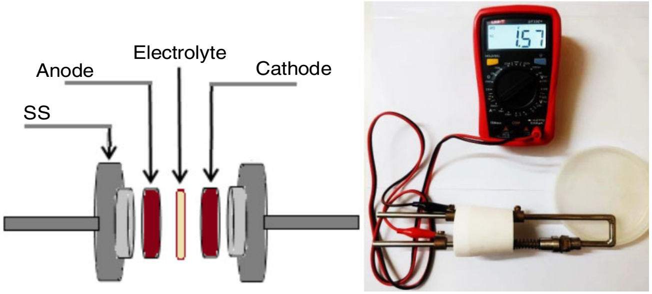

Fig. 8. Schematic assembly for battery configuration and OCV of the cell

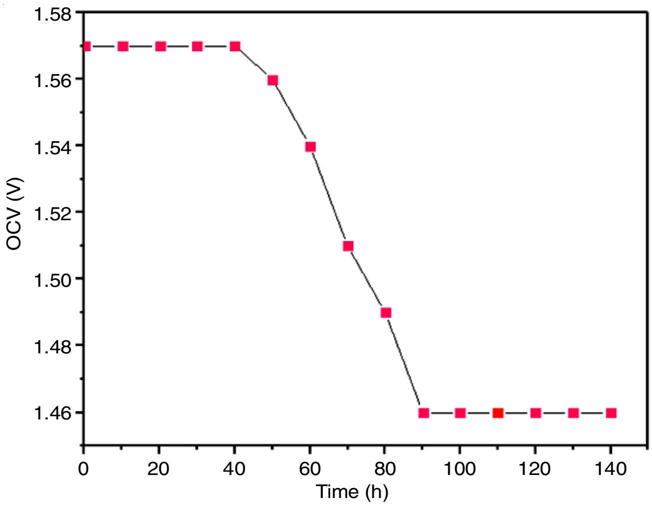

Fig. 9. Discharge characteristics of 80PVP:20PAN:30 wt.% NH_4SCN blend polymer electrolyte

The open circuit voltage (OCV) has been measured and found to be 1.57 V. Zinc has a standard oxidation potential of -0.7618 V, while V_2O_5 has a standard reduction potential of 0.957 V [36]. The cell's OCV has a theoretical value of 1.7188 V. Activation polarization may be to responsible for the difference between the theoretical and experimental values of OCV [17].

Conclusion

A solid polymer blend electrolyte thin film based on polyvinyl pyrrolidone (PVP) and polyacrylonitrile (PAN) complexed with ammonium thiocyanate (NH_4SCN) has been successfully prepared by solution cast technique. The XRD spectrum confirms the amorphous nature of the solid polymer blend electrolytes. The ionic conductivity increased to 6.05×10^{-4} S cm^{-1} with the addition of salt concentrations upto 30 wt.% has been confirmed through EIS analysis. Temperature-dependent ionic conductivity of the prepared polymer blend electrolyte obeys the Arrhenius relationship. The transference number of ion (t_{ion}) and electron (t_e) in the solid polymer blend electrolyte system was found to be 0.976 and 0.023 respectively indicating that the dominancy of ion is responsible for DC ionic conductivity in the polymer blend electrolyte. LSV analysis revealed that the highest conducting SPE PPA@30 were electrochemically stable which confirmed that the prepared SPE is suitable for electrochemical devices. To ensure the maximum possible conductivity, the proton battery was made with SPE PPA@30. Their discharge characteristics were investigated and the open circuit voltage (OCV) was found to be 1.57 V.

ACKNOWLEDGEMENTS

The authors thank UGC-MRP (No.F MRP-5881/15) & DST-FIST for providing research facilities in Madras Christian College, Chennai.

CONFLICT OF INTEREST

The authors declare that there is no conflict of interests regarding the publication of this article.

REFERENCES

1. M. Hema, S. Selvasekarapandian, D. Arunkumar, A. Sakunthala and H. Nithya, *J. Non-Cryst. Solids*, **355**, 84 (2009); https://doi.org/10.1016/j.jnoncrysol.2008.10.009
2. A.L. Saroj and R.K. Singh, *J. Phys. Chem. Solids*, **73**, 162 (2012); https://doi.org/10.1016/j.jpcs.2011.11.012
3. J. Przepiórski, *Mater. Chem. Phys.*, **92**, 1 (2005); https://doi.org/10.1016/j.matchemphys.2005.01.010
4. H. Zhang, X. Ma and D. Yang, *Mater. Lett.*, **58**, 5 (2004); https://doi.org/10.1016/S0167-577X(03)00394-X
5. T.M.W.J. Bandara, D.G.N. Karunathilaka, J.L. Ratnasekera, L.A. De Silva, A.C. Herath and B.E. Mellander, *Ionics*, **23**, 1711 (2017); https://doi.org/10.1007/s11581-017-2016-y
6. T. Si, Y. Ma, Y. Li and D. Liu, *Mater. Chem. Phys.*, **193**, 1 (2017); https://doi.org/10.1016/j.matchemphys.2017.02.004
7. R. Pratap, B. Singh and S. Chandra, *J. Power Sources*, **161**, 702 (2006); https://doi.org/10.1016/j.jpowsour.2006.04.020
8. A.R. Polu and R. Kumar, *Chin. J. Polym. Sci.*, **31**, 641 (2013); https://doi.org/10.1007/s10118-013-1246-3
9. N. Farah, H. Ng, A. Numan, C.-W. Liew, N.A.A. Latip, K. Ramesh and S. Ramesh, *Mater. Sci. Eng. B*, **251**, 114468 (2019); https://doi.org/10.1016/j.mseb.2019.114468
10. B.S. Aziz, R.M. Abdullah, M.A Rasheed and H.M. Ahmed, *Polymers*, **9**, 338 (2017); https://doi.org/10.3390/polym9080338
11. B.S. Aziz, Rawezh B. Marif, M. A. Brza, M. H. Hamsan and M. F. Z. Kadir, *Polymers*, **11**, 1694 (2019); https://doi.org/10.3390/polym11101694
12. J. Wang, S. Song, S. Gao, R. Muchakayala, R. Liu and Q. Ma, *Polym. Test.*, **62**, 278 (2017); https://doi.org/10.1016/j.polymertesting.2017.07.016
13. S.B. Aziz, O.G. Abdullah and A.S. Hussein, *J. Electron. Mater.*, **47**, 3800 (2018); https://doi.org/10.1007/s11664-018-6250-5
14. Z. Osman, Z.A. Ibrahim and A.K. Arof, *Carbohydr. Polym.*, **44**, 167 (2001); https://doi.org/10.1016/S0144-8617(00)00236-8
15. G.G. Gagliardi, A. Ibrahim, D. Borello and A. El-Kharouf, *Molecules*, **25**, 1712 (2020); https://doi.org/10.3390/molecules25071712
16. N. Srivastava and S. Chandra, *Eur. Polym. J.*, **36**, 421 (2000); https://doi.org/10.1016/S0014-3057(99)00056-7
17. A.S. Samsudin, H.M. Lai and M.I.N. Isa, *Electrochim. Acta*, **129**, 1 (2014); https://doi.org/10.1016/j.electacta.2014.02.074
18. N.S. Salleh, S.B. Aziz, Z. Aspanut and M.F.Z. Kadir, *Ionics*, **22**, 2157 (2016); https://doi.org/10.1007/s11581-016-1731-0
19. M.H. Buraidah and A. Arof, *J. Non-Cryst. Solids*, **357**, 3261 (2011); https://doi.org/10.1016/j.jnoncrysol.2011.05.021
20. N.F. Mazuki, A.P.P. Abdul Majeed, Y. Nagao and A.S. Samsudin, *Polym. Test.*, **81**, 106234 (2020); https://doi.org/10.1016/j.polymertesting.2019.106234
21. S.B. Aziz, M.G. Faraj and O.G. Abdullah, *Sci. Rep.*, **8**, 14308 (2018); https://doi.org/10.1038/s41598-018-32662-1
22. A. Arya and A.L. Sharma, Eds.: A.K. Samantara and S. Ratha, Electrochemical Energy Conversion and Storage Systems for Future Sustainability: Technological Advancements, Chap. 3, CRC Press, U.K. (2020).
23. S.B. Aziz, T.J. Woo, M.F.Z. Kadir and H.M. Ahmed, *J. Sci.: Adv. Mater. Devices*, **3**, 1 (2018); https://doi.org/10.1016/j.jsamd.2018.01.002
24. P. TamilSelvi and M. Hema, *Physica B Condensed Matter*, **437**, 53 (2014); https://doi.org/10.1016/j.physb.2013.12.028
25. S.B. Aziz, Z.H.Z. Abidin and A.K. Arof, *Express Polym. Lett.*, **4**, 300 (2010); https://doi.org/10.3144/expresspolymlett.2010.38
26. S.B. Aziz, M.F.Z. Kadir, M.H. Hamsan, H.J. Woo and M.A. Brza, *Sci. Rep.*, **9**, 13163 (2019); https://doi.org/10.1038/s41598-019-49715-8
27. I.M. Noor, *High Perform. Polym.*, **32**, 168 (2020); https://doi.org/10.1177/0954008319890016
28. M. Hema, S. Selvasekerapandian, A. Sakunthala, D. Arunkumar and H. Nithya, *Physica B*, **403**, 2740 (2008); https://doi.org/10.1016/j.physb.2008.02.001
29. S. Ibrahim, S.M. Mohd Yasin, N.M. Nee, R. Ahmad and M.R. Johan, *Solid State Commun.*, **152**, 426 (2012); https://doi.org/10.1016/j.ssc.2011.11.037
30. R. Mishra, N. Baskaran, P.A. Ramakrishna and K.J. Rao, *Solid State Ion.*, **112**, 261 (1998); https://doi.org/10.1016/S0167-2738(98)00209-4
31. A. Arya, M. Sadiq and A.L. Sharma, *Mater. Today Proc.*, **12**, 554 (2019); https://doi.org/10.1016/j.matpr.2019.03.098
32. B.A. Abdulkadir, J.O. Dennis, M.F.B.A. Shukur, M.M.E. Nasef and F. Usman, *Int. J. Electrochem. Sci.*, **16**, 1 (2021); https://doi.org/10.20964/2021.01.34
33. S. Karthikeyan, S. Sikkanthar, S. Selvasekarapandian, D. Arunkumar, H. Nithya and J. Kawamura, *J. Polym. Res.*, **23**, 51 (2016); https://doi.org/10.1007/s10965-016-0952-2
34. X. Wang, Z. Zhang, Z. Tang and Y. Lin, *Mater. Chem. Phys.*, **80**, 1 (2003); https://doi.org/10.1016/S0254-0584(02)00097-4
35. H. Malankar, S.S. Umare, S.S. Bhoga and K. Singh, *Ionics*, **15**, 73 (2009); https://doi.org/10.1007/s11581-008-0229-9
36. K. Mishra, S.A. Hashmi and D.K. Rai, *High Perform. Polym.*, **26**, 672 (2014); https://doi.org/10.1177/0954008314537540